Interface-Assisted Room-Temperature Magnetoresistance in Cu-Phenalenyl-based Magnetic Tunnel Junctions

Neha Jha[1*], Anand Pariyar[2], Tahereh Sadat Parvini[1], Christian Denker[1], Pavan K. Vardhanapu[3], Gonela Vijaykumar[3], Arne Ahrens[4], Tobias Meyer[4], Michael Seibt[4], Nicolae Atodiresei[5], Jagadeesh S. Moodera[6], Swadhin K. Mandal[3], Markus Münzenberg[1]

1. Institut für Physik - Universität Greifswald, Felix-Hausdorff-Straße 6, Greifswald, 17489, Germany
2. Department of Chemistry, School of Physical Sciences, Sikkim University, Tadong-737102, Gangtok, India
3. Department of Chemical Sciences, Indian Institute of Science Education and Research (IISER), Kolkata, 741246, India
4. IV. Physikalisches Institute, Georg-August-Universitat Göttingen, Friedrich-Hund-Platz 1, Göttingen, 37077, Germany
5. Peter Grünberg Institute and Institute for Advanced Simulation, Forschungszentrum Jülich, Wilhelm-Johnen-Straße, 52428 Jülich, Germany
6. Francis Bitter Magnet Laboratory, Plasma Science and Fusion Center and Department of Physics, Massachusetts Institute of Technology, Cambridge, Massachusetts 02139, United States

Abstract

Delocalized carbon-based radical species with unpaired spin, such as phenalenyl (PLY) radical, opened avenues for developing multifunctional organic spintronic devices. Using direct laser writing and the in-situ deposition, we successfully fabricated Cu-PLY, and Zn-PLY based organic magnetic tunnel junctions (OMTJs) with improved morphology and reduced junction area of $3 \times 8\ \mu m^2$. The nonlinear and weakly temperature-dependent current-voltage (I-V) characteristics in combination with the low organic barrier height suggest tunneling as the dominant transport mechanism in the structurally and dimensionally optimized OMTJs. Cu-PLY-based OMTJs, show a significant magnetoresistance up to 14% at room temperature due to the formation of hybrid states at the metal-molecule interfaces called "Spinterface", which reveals the importance of spin-dependent interfacial modification in OMTJs design. Additionally, at high bias in absence of magnetic field, OMTJ shows stable voltage-driven resistive switching. Cu-PLY having spin ½ with net magnetic moment demonstrate the magnetic hardening between the surface molecule at the Co interface and give rise to stable MR suggests their use as feasible and scalable platform for building molecular-scale quantum memristors and processors.

Keywords: organic magnetic tunnel junctions, spinterface induced magnetoresistance, resistive switching, magnetic exchange coupling, direct laser writing, molecular spintronics

Introduction

Organic spintronics, a nascent field at the crossover of spintronics with organic electronics and magnetism, has attracted extensive interest and gradually developed into a new potential platform for future information technologies[1–10] due to the intriguing properties of organic materials such as long-spin coherence times[11–13], tunability of the magnetic properties by molecular design, and high chemical diversity[14]. Organic magnetic tunnel junctions (OMTJs)[15], whereby a thin layer of organic molecules is sandwiched between two ferromagnetic (FM) electrodes, have received immense attention due to their mechanical flexibility, chemically tunable electronic property, and structural fabricability[16–18]. After the first report of magnetoresistance (MR) in an organic junction[19], many groups have reported MR measurement by studying the spin injection and transport in OMTJs with different organic materials[2,5,20–24]. The performance of such devices depends not only on the properties of the organic molecule as the tunnel barrier, and magnetic injecting electrodes, but also spectacularly on the interfacial properties in the hybrid region of devices so-called "spinterface"[3,25]. This region, which arises from orbital hybridization between organic molecules and spin-split bands of the ferromagnet, can drastically influence the spin transport properties of devices. Consequently, the accurate design of the spinterface is crucial and for that some considerations must be made simultaneously, i.e., the energy level alignment for facilitating the carrier injection and the spin injection/extraction, and modification of the magnetic properties of FM electrode/organic molecule interfaces[26].

Extensive investigation has been performed to improve the spinterface and hence the tunnel magnetoresistance (TMR) value in OMTJs[20,27–35]. Despite getting high TMR signal in OMTJ at 2 K[25] and 11 K[1], there are very few reports at room temperature[36]. Main reason being instability of organic molecules at room temperatures, leading to the formation of poor-quality interface between FM and organic molecules. An oxide layer of 1-2 nm is often inserted between the organics and the FM contact to enhance the MR effect[27,37–40], but their transport properties remain unclear. To explore the MR due to interfacial effect between FM and organic materials, there is a strong need to design organic molecules, which forms a stable interface up to room temperature.

Delocalized carbon-based radical molecules with an unpaired free electron, such as phenalenyl (PLY)–based radicals[41,42], provide novel schemes for building organic spintronics devices[43,44], since their spin structure can be manipulated by external stimuli (such as light, electric and magnetic fields). It has been shown that PLY coordinated with zinc ion (ZMP)-based tunnel junction generates 20% MR near room temperature[43,45,46].

These progresses inspired us to explore PLY and its transition metal based complex molecules-based OMTJ, i.e. Cu-PLY. Contrary to the Zn-PLY, Cu-PLY is a typical coordination complex hence Cu-PLY is air and moisture stable. This being one of the main reasons to explore this molecule system. Furthermore, Cu-PLY is paramagnetic ($\chi>0$) with spin ½ net magnetic

moment, therefore, the interaction of these molecules with the magnetic field would be different. Therefore, Cu-PLY is expected to modify interaction at the interface, and influence the spin transport. For this purpose, we developed three-dimensional (3D) mask with two-photon absorption lithography (TPL)[47]. Low temperature (LT) ~ 80K, in-situ UHV angle deposition method combined with 3D-mask was used to fabricate OMTJs with an effective area of $3 \times 8\ \mu m^2$. These devices show MR ratio $\sim 10 - 14\%$ without the use of oxide layers between FM/organic interface at room temperature, which is to our knowledge is one of the highest MR ratios reported [48–50].

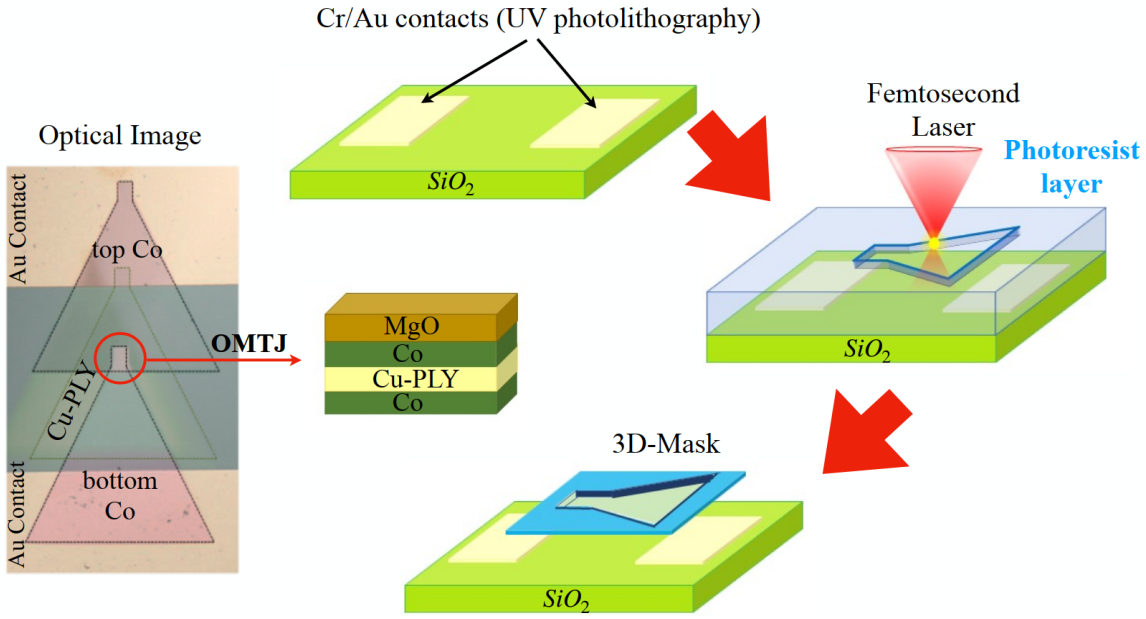

Figure1: Schematic of three-dimensional mask writing process using two-photon absorption lithography. Optical image (left) of the segment used to prepare single OMTJ with top and bottom Co electrodes and resulting stack layer.

Fabrication and Optimization of OMTJs

We used TPL technique to fabricate 3D masks. The steps of the fabrication process are shown in Figure 1. The use of 3D mask ensures precise control of the cross-sectional dimensions as well as tuning the overall size of 3D molecular junctions. Using the 3D mask and angle deposition method as explained in the supporting information (SI) (SI Figure S-3) we fabricated multiple sets of wedge devices (SI Figure S-4) in two different categories. In the first category, wedge devices consist Co(8 nm)/PLY(Cu, Zn, 2-6 nm)/Co(12 nm)/MgO(4 nm), and in the second Co(8 nm)/Cu-PLY(2-6 nm)/Cu(12nm)/MgO (4 nm). In the latter, we replaced top magnetic electrodes with non-magnetic Copper electrode. Here, a thin layer of MgO ($\approx$ 4 nm) works as a capping layer to protect the devices from degrading due to the interaction with the environment. Co/Cu electrodes and the capping layers were deposited by e-beam evaporation. The organic materials were deposited by thermal evaporation with substrate temperature of ~ 80 K. Optical image of a single OMTJ, having two Co electrodes with an organic barrier layer is shown in Figure 1. The area was decreased by a

factor of $10^3 - 10^4$, through the 3D printing of the mask and the new shadow evaporation technique, demonstrated for the first time.

The structure of PLY and its transition-metal-based complex molecules (Cu-PLY and ZMP) are shown in Figure 2(a). To get a working MTJ, a very thin barrier layer is required, since tunneling is expected to dominate in thin barrier junctions and decays exponentially with increasing thickness[51].

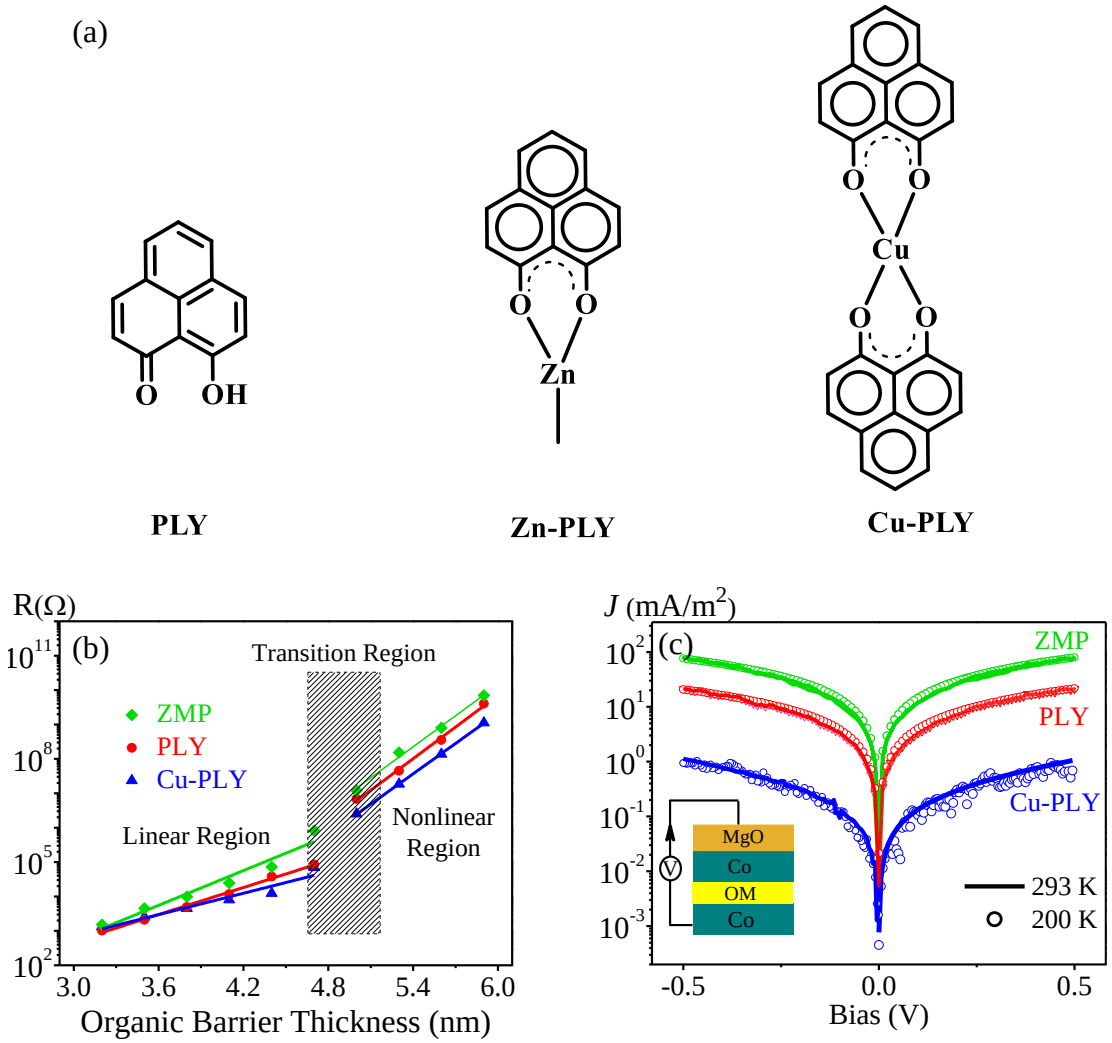

Figure 2: (a) Structure of phenalenyl and its transition metal based complex molecules. (b) Variation of the resistance as a function of the organic barrier thickness, and (c) current density versus bias voltage for OMTJs with different organic molecules at temperatures 200 K (dotted lines) and 293 K (slid line).

In Figure 2(b), the resistance of the OMTJs are plotted as a function of the thickness of the different organic layers. Accordingly, for barrier layer thickness below ≈ 2.5 nm resistance is low (100-200 Ω), because of short-circuits via pinholes or diffusion of top electrodes in the organic layer. The abrupt resistance jumps from kΩ to MΩ occurs at thickness ≈ 4.4 nm, afterward by increasing the thickness up to ≈ 6 nm, the resistance increases linearly in logarithmic scale from kΩ to GΩ.

For a thickness more than ≈ 6 nm, the resistance is in the range of more than 100 GΩ, with almost no detectable current below 1V bias. With this optimization, the organic barrier thickness of ≈ 5 nm is selected for the OMTJ device.

In order to get more insight into the origin of spin transport through organic layers, we performed current-voltage (I-V) curves in the low-voltage range at 200 K and 293 K, using a home-built four-point probe cryostat setup. In general, the spin-dependent transport phenomenon in OMTJs is governed by tunneling and hopping mechanisms[38–40]. Inspection of the data in Figure 2(b) and 2(c) reveals that for organic-layer thickness ranging of $\approx 4.7 - 5.6$ nm, the J-V curves are clearly non-linear and symmetric, and resistance has a weak temperature dependence with negligible resistance variation at 293 K and 200 K. This excludes the thermally activated hopping as the dominating transport mechanism. The J-V curves of OMTJ junctions with area A (J = I/A) are well-matched with the theoretical Brinkman model[52] based on the Wentzel− Kramers−Brillouin (WKB) approximation for estimation of barrier height "ϕ"(eV) and tunneling barrier thickness "d" (nm) (details see in SI table S1). These results clearly shows that the tunneling is the dominating transport mechanism in the optimized OMTJs discussed in this report.

Tunneling magnetoresistance (TMR) of Cu-PLY-based OMTJs

To further explore the spin transport properties of our OMTJs, we focus to investigate the TMR with Cu-PLY molecule being the barrier layer. Cu-PLY synthesis and its characterization is explained in SI Figure S-1 and S-2, and Figure S-9 to S-13 and crystallography details are given in table S2 to table S5. In such systems, the TMR arises from the magnetization-dependent total density of states of the tunneling electrons at the surface[45]. The Transmission electron microscopy (TEM) images of Cu-PLY-based OMTJs show that all the interfaces are sharp and without interdiffusion, see Figure 3(a). The nonlinear I–V characteristics with $\phi = 1.32$ eV suggest tunneling as the dominant transport mechanism, see Figure 3(b). Moreover, the magnetic properties of the OMTJ were characterized using magneto-optical Kerr effect (MOKE) measurement technique at room temperature. The hysteresis loops for the top and bottom electrodes of the device in Figure 3(c) shows coercive field of $H_c \sim 10$ mT and $H_c \sim 15$ mT, respectively, although as we showed in SI Figure S-5, for 8 nm Co thin film $H_c \sim 6$ mT. This suggests that addition of Cu-PLY layer enhances the coercivity/switching field of Co (also with ZMP and PLY shown in SI S-5). A significant change in the MOKE curve is a signature of the molecules anisotropy. The magnetic moment/coercive field modification depend strongly on the hybridization between the π-electrons of the Cu-PLY molecular layers and the 3d-band electrons of the Co metal. Furthermore, as a result of the hybridization, the electronic states at the interface change, leading to a new hybrid interface called "Spinterface"[3,25].

Variation of the resistance as a function of the in-plane magnetic field amplitude is shown in Figure 3(d). The TMR can be defined as $\mathrm{TMR} = (R_{AP} - R_P)/R_P \times 100$, where R_P and R_{AP} are the

tunneling resistance when magnetization of the two electrodes are aligned in parallel (p) and antiparallel (AP), respectively. We found TMR ~ 14% for Cu-PLY-based OMTJ, which lies among the highest value obtained until now in a device without adding any oxide tunnel barrier between FM/organic interface at room temperature (to compare MR results, PLY and ZMP based OMTJ shown in SI Figure S-7). This is a promising finding for the development of future logic devices by increasing the material choice as it is very limited in present.

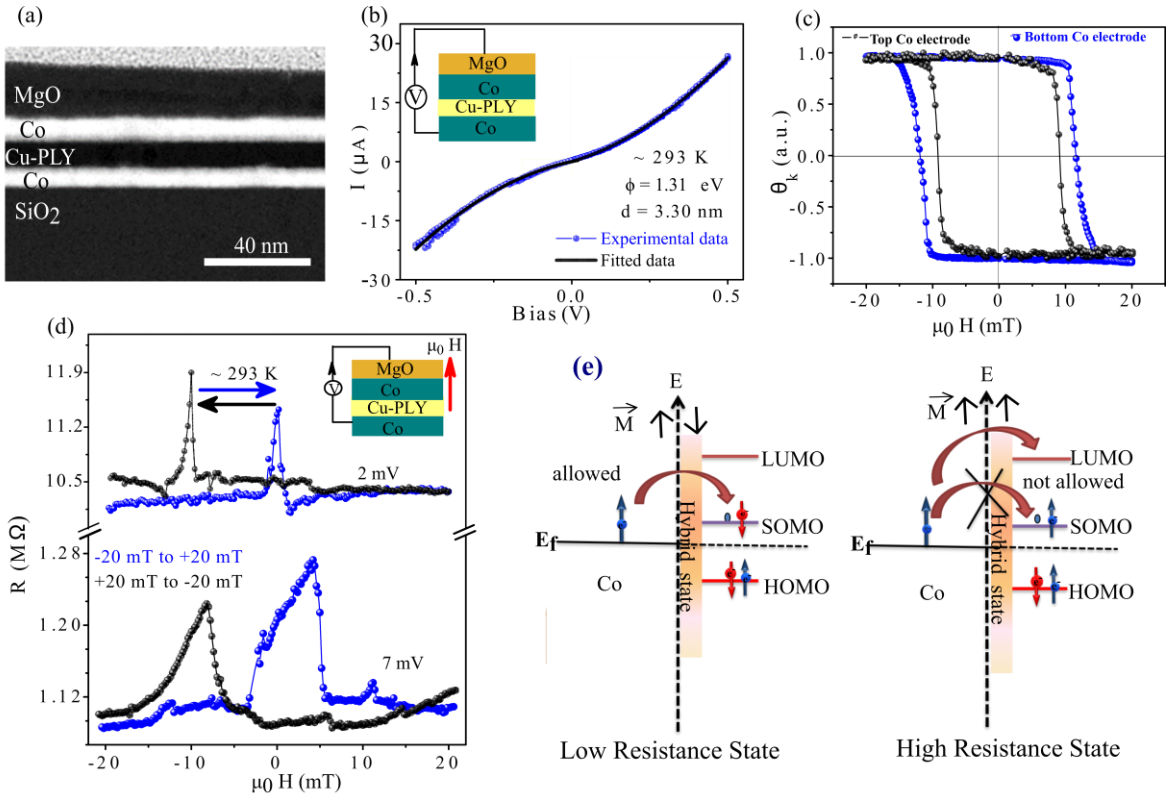

Figure 3: (a) TEM image of junction showing sharp interface without any diffusion of interlayer. (b) Non-linear I-V at room temperature. (c) Hysteresis loop of the OMTJ shows a switching field near 10 mT. (d) MR measurement with two different applied bias voltages, top for 2 mV and bottom for 7 mV. (e) Model explaining low and high resistance state of OMTJ devices (adapted from K.V Raman[53]).

To understand the mechanism behind TMR signal with Cu-PLY OMTJs, we used a model similar to the one discussed in Raman *et al.*[53] as the Cu-PLY molecule is planar molecular (crystallographic picture see in SI Figure S-10) like ZMP. The origin of the MR signal can be explained based on the spin selective transport through the hybrid interface (see Figure 3(e)). Figure 3(e) shows schematically the Co Fermi level (E_f) and the lowest unoccupied molecular orbitals (LUMO), highest occupied molecular orbitals (HOMO), and semi occupied molecular orbitals (SOMO) of radical state of the Cu-PLY molecule. As the HOMO is fully occupied, the SOMO of the molecule with a free electron with spin up or down participates in transport. It is very well established that the SOMO of the odd alternant hydrocarbon PLY-based radical is

formally a nonbonding molecular orbital (NBMO) and hence during transport it experiences a minimal change in reorganization energy[54]. Due to the strong exchange bias coupling of the Cu-PLY molecule to Co surface (as we see in Figure 3(c)) a new hybrid interface is formed. When the spin of Co and the SOMO level of this hybrid molecular interface are aligned anti-parallel (Figure 3(e) left), the spin-up electron from metal can be injected into the SOMO hence showing lower resistance. On the other hand, when the Co layer and the interface layer are aligned parallel (Figure 3(e) right), absence of required empty spin state in the SOMO level of the hybrid molecular interface requires tunneling via LUMO, which leads to higher resistive state. Theoretical calculations and atomic scale experiments (STM measurements)[55] demonstrated that by chemisorbing organic molecules containing metal atoms onto a magnetic substrate a spin unbalanced interaction is induced into the π-orbitals molecular orbitals and metal d-states. As a consequence, the chemisorbed molecule acts as an efficient spin-filter[45,56,57]. Consequently, the Cu-PLY layer can be a spin filter with a high MR effect at room temperature.

To further explore the spinterface properties, we replace the top magnetic electrode with a non-magnet Cu electrode which gives interface induced MR. Figure 4(a) shows independent switching of the bottom Co with respect to the hybridized interface layer giving rise to the Interface magnetoresistance (IMR) effect. This happens due to the strong π-d hybridization between molecular π −orbitals and the Co d-states which alter magnetic properties of Co surface[3]. IMR ratio IMR = $(R_{AP} - R_P)/R_P \times 100 \sim 10\%$, where R_P (as see in Figure 4(a), $R_P = \frac{R_{P1}+R_{P2}}{2}$) and R_{AP} are the resistance when magnetization of Co electrode and interface are aligned in P and AP states, respectively.

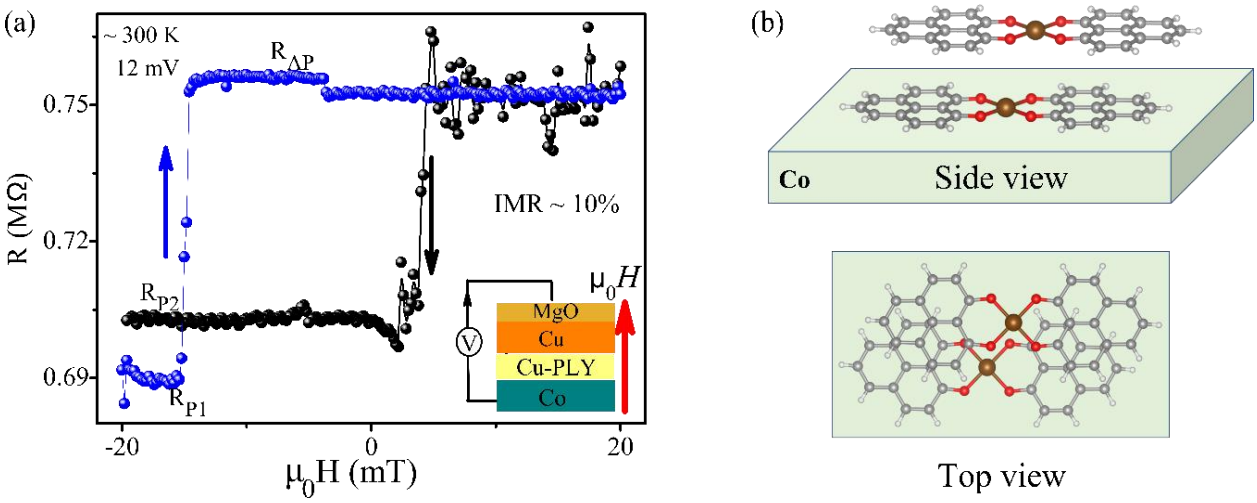

Figure 4: (a) Resistance variation with applied magnetic field for OMTJ Co/Cu-PLY/Cu/MgO at room temperature showing IMR effect. (b) Schematic of 2 layers of Cu-PLY adsorption (top image) on Co surface (side view) and bottom image shows top view of Cu-PLY molecular structure adsorbs on Co surface.

The interaction of the PLY part of the molecule with the Co substrate is rather similar like when Zn-PLY system interacts with Co surface[43]. In in Figure 4(b), top schematic showing the adsorption of Cu-PLY molecule (which is planar molecules) on Co surface. The PLY ligand

chemisorbs on the magnetic substrate due to the strong hybridization between the π- orbitals of the PLY-ligand and *d*-states of Co surface atoms shown. More precisely, in case of other π-conjugated molecules or graphene flakes that interact with magnetic surfaces and magnetic exchange interactions drastically increase and giving rise an intra-layer magnetic hardening[58–60] leading to the formation of nanomagnets embedded into the magnetic substrates. Interestingly, this hybrid molecule-surface nanomagnets can switch independently with respect to the surrounding magnetic substrate[43,58,61] and represents also a key effect for the new devices discussed in this work. It is worth mentioning that by controlling the Co/Cu-PLY hybrid interface, spinterface effect higher IMR could be accessible. We found evidence that multiple 100% IMR could potentially be realized, consistent with spinterface owning a spin blockade effect.

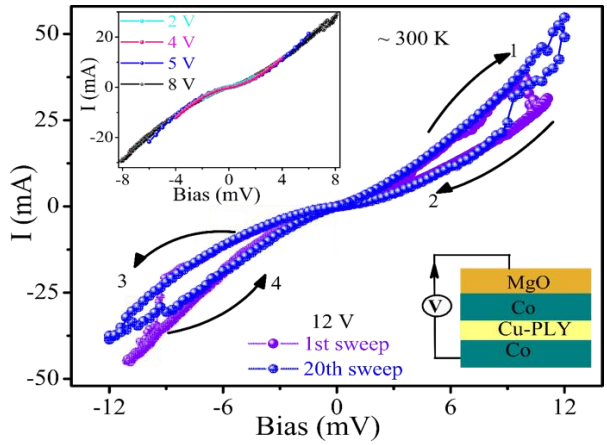

Figure: 5 I-V room temperature characteristics at H = 0. The irreversibility is clearly visible at both positive and negative voltages (bias). Inset: I-V characteristics from 3 V to 8 V reflect that at low voltage range there is no hysteresis appeared.

Additionally, with the MR effect, as shown in Figure 5, the I–V characteristics of Co/Cu-PLY/Co junction demonstrate a novel preliminary electric memory effect. By increasing the bias voltage from zero to positive voltages, it can be seen that the device is in a low conductivity state with less than half of the resistance. Current sharply increases from 20 mA to 50 mA. Within a hysteresis, when the voltage is decreased back to zero, the device returns to the high conductance state. A similar process occurs at negative voltages. This I-V behavior at high bias, indicates that the device resistance can increase or decrease depending on the polarity of bias voltage. This hysteresis behavior exhibits a typical "pinch-off"[62] feature like in memristive devices similarly shown in Bandyopadhyay *et. al*[63], operated at different voltage levels with different current responses. The continuous multiple sweep (for 20 cycle) measurements return no significant degradation in the performance of the OMTJs, which indicates their stable behavior. Furthermore, voltage-driven resistance switching phenomena has several mechanisms in different molecular spintronic devices[64–66]. In this case, OMTJ based memristive devices change their resistance by varying the direction of the spin of the electron. Not only Cu-Ply but also PLY and ZMP show the similar

switching effect (see SI Figure S-8). The final device magnetization state is determined by the accumulative effect of electrons and spin excitations. Thus, device conductance/current depends also on the integral effects of the I-V profile. For the device that means the MR effect is always connected to memory effects in molecular layer.

Conclusion

Using 3D mask and low temperature in-situ deposition, we successfully fabricate PLY, Cu-PLY, and Zn-PLY based OMTJs without adding any additional interface separation. With optimal tunnel barrier thickness of ~ 5 nm, our studies (I-V) have shown tunneling as the dominant electron/spin transport mechanism in optimized OMTJs. By tuning the function of the PLY-molecule by their chemistry, by adding Cu at the center of the molecule i.e., with Cu-PLY, evidently changes the interface coupling and magnetic anisotropy is observed. We find room temperature TMR $\sim 14\%$ for OMTJs, which lies among the highest values reported so far in devices without oxide layer at metal/molecule interface, and OMTJ with Cu top electrode show IMR$\sim 10\ \%$. We demonstrate a memristive behavior at higher voltages, allowing to manipulate the interface charge in future works. The memristive aspect is completely new and a very exciting result and directly related to the properties of the interfacial nature of the molecule. Most importantly, our results demonstrate the potential for controlling parameters such as the sign and magnitude of magnetoresistance by engineering the interfacial properties represent an ideal material platform to develop high quality spinterface effects. Having these finding, pave the way for the development of room temperature molecular memory logic and memristor devices.

Acknowledgments

This work was supported by the Landesgraduiertenfördung Mecklenburg-Vorpommern and by the Deutsche Forschung gemeinschaft (DFG, German Research Foundation). N.J gratefully acknowledges funding by the LGF. J.S.M thanks NSF support (DMR-2218550, CIQM-NSF DMR-1231319), and ARO grant W911NF-20-2-0061. N.A. acknowledge DFG support within CRC1238, Project No. 277146874 - CRC 1238 (subproject C01). I would like to acknowledge Dr. Alessandro Lodesani and Dr. Vibhuti Rai for fruitful discussion.

Contribution

M.M and S.K.M designed the original research approach of this work. M.M, C.D and N.J conceived the idea of study spin dependent transport on OMTJ. C.D and N.J design the experiment and fabrication of devices with 3D mask technology. N.J carried out the experiments. N.J, C.D, and J.S.M analyzed the data. N.J, M.M, and T.P wrote the manuscript including contribution from all the authors. A.P synthesized the Cu-PLY molecule, V.G and P.K.V characterized the Cu-PLY molecule by single crystal X-ray, P.K.V prepared PLY, Zn-PLY and Cu-PLY molecules. N.A provides supporting qualitative theory for Co/Cu-PLY hybrid system. S.K.M supervised the molecular materials preparation and characterization. A.A and T.M and M.S carried out TEM measurements.

Authors declared no competing interest.

ASSOCIATED CONTENT

* Supporting Information

Cu-PLY synthesis methods, crystal structure and characterization data are available in SI. Fabrication method of 3D mask and in-situ low temperature OMTJ growth and initial electrical and magnetic properties shown in SI. Resistive switching of PLY and ZMP is also observed and shown in SI.

Corresponding Authors

*Neha Jha, Email: nehamiranda18@gmail.com,

*Dr. Nicolae Atodiresei, Email: n.atodiresei@fz-juelich.de

References

(1) Dediu, V. A.; Hueso, L. E.; Bergenti, I.; Taliani, C. Spin Routes in Organic Semiconductors. *Nat. Mater.* **2009**, *8* (9), 707–716. https://doi.org/10.1038/nmat2510.

(2) Xiong, Z. H.; Wu, D.; Valy Vardeny, Z.; Shi, J. Giant Magnetoresistance in Organic Spin-Valves. *Nature* **2004**, *427* (6977), 821–824. https://doi.org/10.1038/nature02325.

(3) Sanvito, S. The Rise of Spinterface Science. *Nat. Phys.* **2010**, *6* (8), 562–564. https://doi.org/10.1038/nphys1714.

(4) Tran, T. L. A.; Çakır, D.; Wong, P. K. J.; Preobrajenski, A. B.; Brocks, G.; van der Wiel, W. G.; de Jong, M. P. Magnetic Properties of Bcc-Fe(001)/C 60 Interfaces for Organic Spintronics. *ACS Appl. Mater. Interfaces* **2013**, *5* (3), 837–841. https://doi.org/10.1021/am3024367.

(5) Shim, J. H.; Raman, K. V; Park, Y. J.; Santos, T. S.; Miao, G. X.; Satpati, B.; Moodera, J. S. Large Spin Diffusion Length in an Amorphous Organic Semiconductor. *Phys. Rev. Lett.* **2008**, *100* (22), 226603. https://doi.org/10.1103/PhysRevLett.100.226603.

(6) CHAPPERT, C.; FERT, A.; VAN DAU, F. N. The Emergence of Spin Electronics in Data Storage. In *Nanoscience and Technology*; Co-Published

with Macmillan Publishers Ltd, UK, 2009; Vol. 6, pp 147–157. https://doi.org/10.1142/9789814287005_0015.

(7) Lehmann, J.; Gaita-Ariño, A.; Coronado, E.; Loss, D. Quantum Computing with Molecular Spin Systems. *J. Mater. Chem.* **2009**, *19* (12), 1672–1677. https://doi.org/10.1039/B810634G.

(8) Bergenti, I.; Dediu, V.; Prezioso, M.; Riminucci, A. Organic Spintronics. *Philos. Trans. R. Soc. A Math. Phys. Eng. Sci.* **2011**, *369* (1948), 3054–3068. https://doi.org/10.1098/rsta.2011.0155.

(9) de Jong, M. P. Recent Progress in Organic Spintronics. *Open Phys.* **2016**, *14* (1), 337–353. https://doi.org/10.1515/phys-2016-0039.

(10) Kulkarni, A. P.; Tonzola, C. J.; Babel, A.; Jenekhe, S. A. Electron Transport Materials for Organic Light-Emitting Diodes. *Chem. Mater.* **2004**, *16* (23), 4556–4573. https://doi.org/10.1021/cm049473l.

(11) Fert, A. Origin, Development, and Future of Spintronics (Nobel Lecture). *Angew. Chemie Int. Ed.* **2008**, *47* (32), 5956–5967. https://doi.org/10.1002/anie.200801093.

(12) Sanvito, S.; Rocha, A. R. Molecular-Spintronics: The Art of Driving Spin Through Molecules. *J. Comput. Theor. Nanosci.* **2006**, *3* (5), 624–642. https://doi.org/10.1166/jctn.2006.3047.

(13) Morita, Y.; Suzuki, S.; Sato, K.; Takui, T. Synthetic Organic Spin Chemistry for Structurally Well-Defined Open-Shell Graphene Fragments. *Nat. Chem.* **2011**, *3* (3), 197–204. https://doi.org/10.1038/nchem.985.

(14) Ding, S.; Tian, Y.; Li, Y.; Zhang, H.; Zhou, K.; Liu, J.; Qin, L.; Zhang, X.; Qiu, X.; Dong, H.; Zhu, D.; Hu, W. Organic Single-Crystal Spintronics: Magnetoresistance Devices with High Magnetic-Field Sensitivity. *ACS Nano* **2019**, *13* (8), 9491–9497. https://doi.org/10.1021/acsnano.9b04449.

(15) Sato, H.; Enobio, E. C. I.; Yamanouchi, M.; Ikeda, S.; Fukami, S.; Kanai, S.; Matsukura, F.; Ohno, H. Properties of Magnetic Tunnel Junctions with a MgO/CoFeB/Ta/CoFeB/MgO Recording Structure down to Junction Diameter of 11 Nm. *Appl. Phys. Lett.* **2014**, *105* (6), 062403. https://doi.org/10.1063/1.4892924.

(16) Wang, F. J.; Yang, C. G.; Vardeny, Z. V.; Li, X. G. Spin Response in Organic Spin Valves Based on La2/3Sr1/3MnO3 Electrodes. *Phys. Rev. B* **2007**, *75* (24), 245324. https://doi.org/10.1103/PhysRevB.75.245324.

(17) Gorjizadeh, N.; Quek, S. Y. Interface Effects on Tunneling Magnetoresistance in Organic Spintronics with Flexible Amine–Au Links. *Nanotechnology* **2013**, *24* (41), 415201. https://doi.org/10.1088/0957-4484/24/41/415201.

(18) Mahato, R. N.; Lülf, H.; Siekman, M. H.; Kersten, S. P.; Bobbert, P. A.; de Jong, M. P.; De Cola, L.; van der Wiel, W. G. Ultrahigh Magnetoresistance at Room Temperature in Molecular Wires. *Science (80-.).* **2013**, *341* (6143), 257–260. https://doi.org/10.1126/science.1237242.

(19) Dediu, V.; Murgia, M.; Matacotta, F. C.; Taliani, C.; Barbanera, S. Room Temperature Spin Polarized Injection in Organic Semiconductor. *Solid State Commun.* **2002**, *122* (3–4), 181–184. https://doi.org/10.1016/S0038-1098(02)00090-X.

(20) Santos, T. S.; Lee, J. S.; Migdal, P.; Lekshmi, I. C.; Satpati, B.; Moodera, J. S. Room-Temperature Tunnel Magnetoresistance and Spin-Polarized Tunneling through an Organic Semiconductor Barrier. *Phys. Rev. Lett.* **2007**, *98* (1), 016601. https://doi.org/10.1103/PhysRevLett.98.016601.

(21) Sun, D.; Yin, L.; Sun, C.; Guo, H.; Gai, Z.; Zhang, X.-G.; Ward, T. Z.; Cheng, Z.; Shen, J. Giant Magnetoresistance in Organic Spin Valves. *Phys. Rev. Lett.* **2010**, *104* (23), 236602. https://doi.org/10.1103/PhysRevLett.104.236602.

(22) Wu, D.; Xiong, Z.; Li, X.; Vardeny, Z.; Shi, J. Magnetic-Field-Dependent Carrier Injection at La2/3Sr1/3MnO3/ and Organic Semiconductors Interfaces. *Phys. Rev. Lett.* **2005**, *95* (1), 016802. https://doi.org/10.1103/PhysRevLett.95.016802.

(23) Chan, Y.-L.; Hung, Y.-J.; Wang, C.-H.; Lin, Y.-C.; Chiu, C.-Y.; Lai, Y.-L.; Chang, H.-T.; Lee, C.-H.; Hsu, Y. J.; Wei, D. H. Magnetic Response of an Ultrathin Cobalt Film in Contact with an Organic Pentacene Layer. *Phys. Rev. Lett.* **2010**, *104* (17), 177204. https://doi.org/10.1103/PhysRevLett.104.177204.

(24) Tokuc, H.; Oguz, K.; Burke, F.; Coey, J. M. D. Magnetoresistance in CuPc Based Organic Magnetic Tunnel Junctions. *J. Phys. Conf. Ser.* **2011**, *303* (1), 012097. https://doi.org/10.1088/1742-6596/303/1/012097.

(25) Barraud, C.; Seneor, P.; Mattana, R.; Fusil, S.; Bouzehouane, K.; Deranlot, C.; Graziosi, P.; Hueso, L.; Bergenti, I.; Dediu, V.; Petroff, F.; Fert, A. Unravelling the Role of the Interface for Spin Injection into Organic

Semiconductors. *Nat. Phys.* **2010**, *6* (8), 615–620. https://doi.org/10.1038/nphys1688.

(26) Sun, Z.; Zhan, Y.; Shi, S.; Fahlman, M. Energy Level Alignment and Interactive Spin Polarization at Organic/Ferromagnetic Metal Interfaces for Organic Spintronics. *Org. Electron.* **2014**, *15* (9), 1951–1957. https://doi.org/10.1016/j.orgel.2014.05.021.

(27) Dediu, V.; Hueso, L. E.; Bergenti, I.; Riminucci, A.; Borgatti, F.; Graziosi, P.; Newby, C.; Casoli, F.; De Jong, M. P.; Taliani, C.; Zhan, Y. Room-Temperature Spintronic Effects in Alq3 -Based Hybrid Devices. *Phys. Rev. B - Condens. Matter Mater. Phys.* **2008**, *78* (11), 115203. https://doi.org/10.1103/PhysRevB.78.115203.

(28) Yoshida, K.; Hamada, I.; Sakata, S.; Umeno, A.; Tsukada, M.; Hirakawa, K. Gate-Tunable Large Negative Tunnel Magnetoresistance in Ni–C 60 –Ni Single Molecule Transistors. *Nano Lett.* **2013**, *13* (2), 481–485. https://doi.org/10.1021/nl303871x.

(29) Schmaus, S.; Bagrets, A.; Nahas, Y.; Yamada, T. K.; Bork, A.; Bowen, M.; Beaurepaire, E.; Evers, F.; Wulfhekel, W. Giant Magnetoresistance through a Single Molecule. *Nat. Nanotechnol.* **2011**, *6* (3), 185–189. https://doi.org/10.1038/nnano.2011.11.

(30) Cucinotta, G.; Poggini, L.; Pedrini, A.; Bertani, F.; Cristiani, N.; Torelli, M.; Graziosi, P.; Cimatti, I.; Cortigiani, B.; Otero, E.; Ohresser, P.; Sainctavit, P.; Dediu, A.; Dalcanale, E.; Sessoli, R.; Mannini, M. Tuning of a Vertical Spin Valve with a Monolayer of Single Molecule Magnets. *Adv. Funct. Mater.* **2017**, *27* (42), 1703600. https://doi.org/10.1002/adfm.201703600.

(31) Cinchetti, M.; Dediu, V. A.; Hueso, L. E. Activating the Molecular Spinterface. *Nat. Mater.* **2017**, *16* (5), 507–515. https://doi.org/10.1038/nmat4902.

(32) Li, D.; Dappe, Y. J.; Smogunov, A. Perfect Spin Filtering by Symmetry in Molecular Junctions. *Phys. Rev. B* **2016**, *93* (20), 201403. https://doi.org/10.1103/PhysRevB.93.201403.

(33) Smogunov, A.; Dappe, Y. J. Symmetry-Derived Half-Metallicity in Atomic and Molecular Junctions. *Nano Lett.* **2015**, *15* (5), 3552–3556. https://doi.org/10.1021/acs.nanolett.5b01004.

(34) Hsu, C.-H.; Chu, Y.-H.; Lu, C.-I.; Hsu, P.-J.; Chen, S.-W.; Hsueh, W.-J.;

Kaun, C.-C.; Lin, M.-T. Spin-Polarized Transport through Single Manganese Phthalocyanine Molecules on a Co Nanoisland. *J. Phys. Chem. C* **2015**, *119* (6), 3374–3378. https://doi.org/10.1021/jp510930y.

(35) Wang, B.; Li, J.; Yu, Y.; Wei, Y.; Wang, J.; Guo, H. Giant Tunnel Magneto-Resistance in Graphene Based Molecular Tunneling Junction. *Nanoscale* **2016**, *8* (6), 3432–3438. https://doi.org/10.1039/C5NR06585B.

(36) Zhang, X.; Tong, J.; Zhu, H.; Wang, Z.; Zhou, L.; Wang, S.; Miyashita, T.; Mitsuishi, M.; Qin, G. Room Temperature Magnetoresistance Effects in Ferroelectric Poly(Vinylidene Fluoride) Spin Valves. *J. Mater. Chem. C* **2017**, *5* (21), 5055–5062. https://doi.org/10.1039/C7TC00517B.

(37) Schoonus, J. J. H. M.; Lumens, P. G. E.; Wagemans, W.; Kohlhepp, J. T.; Bobbert, P. A.; Swagten, H. J. M.; Koopmans, B. Magnetoresistance in Hybrid Organic Spin Valves at the Onset of Multiple-Step Tunneling. *Phys. Rev. Lett.* **2009**, *103* (14), 146601. https://doi.org/10.1103/PhysRevLett.103.146601.

(38) Lin, R.; Wang, F.; Rybicki, J.; Wohlgenannt, M.; Hutchinson, K. A. Distinguishing between Tunneling and Injection Regimes of Ferromagnet/Organic Semiconductor/Ferromagnet Junctions. *Phys. Rev. B* **2010**, *81* (19), 195214. https://doi.org/10.1103/PhysRevB.81.195214.

(39) Gobbi, M.; Golmar, F.; Llopis, R.; Casanova, F.; Hueso, L. E. Room-Temperature Spin Transport in C60-Based Spin Valves. *Adv. Mater.* **2011**, *23* (14), 1609–1613. https://doi.org/10.1002/adma.201004672.

(40) Tran, T. L. A.; Le, T. Q.; Sanderink, J. G. M.; van der Wiel, W. G.; de Jong, M. P. The Multistep Tunneling Analogue of Conductivity Mismatch in Organic Spin Valves. *Adv. Funct. Mater.* **2012**, *22* (6), 1180–1189. https://doi.org/10.1002/adfm.201102584.

(41) Itkis, M. E.; Chi, X.; Cordes, A. W.; Haddon, R. C. Magneto-Opto-Electronic Bistability in a Phenalenyl-Based Neutral Radical. *Science (80-.).* **2002**, *296* (5572), 1443–1445. https://doi.org/10.1126/science.1071372.

(42) Roy, S. R.; Nijamudheen, A.; Pariyar, A.; Ghosh, A.; Vardhanapu, P. K.; Mandal, P. K.; Datta, A.; Mandal, S. K. Phenalenyl in a Different Role: Catalytic Activation through the Nonbonding Molecular Orbital. *ACS Catal.* **2014**, *4* (12), 4307–4319. https://doi.org/10.1021/cs5010695.

(43) Raman, K. V; Kamerbeek, A. M.; Mukherjee, A.; Atodiresei, N.; Sen, T. K.;

Lazić, P.; Caciuc, V.; Michel, R.; Stalke, D.; Mandal, S. K.; Blügel, S.; Münzenberg, M.; Moodera, J. S. Interface-Engineered Templates for Molecular Spin Memory Devices. *Nature* **2013**, *493* (7433), 509–513. https://doi.org/10.1038/nature11719.

(44) Moodera, J. S.; Koopmans, B.; Oppeneer, P. M. On the Path toward Organic Spintronics. *MRS Bull.* **2014**, *39* (7), 578–581. https://doi.org/10.1557/mrs.2014.128.

(45) Atodiresei, N.; Brede, J.; Lazić, P.; Caciuc, V.; Hoffmann, G.; Wiesendanger, R.; Blügel, S. Design of the Local Spin Polarization at the Organic-Ferromagnetic Interface. *Phys. Rev. Lett.* **2010**, *105* (6), 066601. https://doi.org/10.1103/PhysRevLett.105.066601.

(46) Raman, K. V. Interface-Assisted Molecular Spintronics. *Appl. Phys. Rev.* **2014**, *1* (3), 031101. https://doi.org/10.1063/1.4890496.

(47) Farsari, M.; Chichkov, B. N. Two-Photon Fabrication. *Nat. Photonics* **2009**, *3* (8), 450–452. https://doi.org/10.1038/nphoton.2009.131.

(48) Ding, S.; Tian, Y.; Li, Y.; Mi, W.; Dong, H.; Zhang, X.; Hu, W.; Zhu, D. Inverse Magnetoresistance in Polymer Spin Valves. *ACS Appl. Mater. Interfaces* **2017**, *9* (18), 15644–15651. https://doi.org/10.1021/acsami.7b02804.

(49) Yao, X.; Duan, Q.; Tong, J.; Chang, Y.; Zhou, L.; Qin, G.; Zhang, X. Magnetoresistance Effect and the Applications for Organic Spin Valves Using Molecular Spacers. *Materials (Basel).* **2018**, *11* (5), 721. https://doi.org/10.3390/ma11050721.

(50) Li, D.; Yu, G. Innovation of Materials, Devices, and Functionalized Interfaces in Organic Spintronics. *Adv. Funct. Mater.* **2021**, *31* (28), 2100550. https://doi.org/10.1002/adfm.202100550.

(51) Butler, W. H.; Zhang, X.-G.; Schulthess, T. C.; MacLaren, J. M. Spin-Dependent Tunneling Conductance of $\mathrm{Fe}|\mathrm{MgO}|\mathrm{Fe}$ Sandwiches. *Phys. Rev. B* **2001**, *63* (5), 54416. https://doi.org/10.1103/PhysRevB.63.054416.

(52) Brinkman, W. F.; Dynes, R. C.; Rowell, J. M. Tunneling Conductance of Asymmetrical Barriers. *J. Appl. Phys.* **1970**, *41* (5), 1915–1921. https://doi.org/10.1063/1.1659141.

(53) Raman, K. V. Spin Injection and Transport in Organic Semiconductors, PhD

thesis, MIT, 2011. https://doi.org/http://dspace.mit.edu/handle/1721.1/7582.

(54) HADDON, R. C. Design of Organic Metals and Superconductors. *Nature* **1975**, *256* (5516), 394–396. https://doi.org/10.1038/256394a0.

(55) Brede, J.; Atodiresei, N.; Kuck, S.; Lazić, P.; Caciuc, V.; Morikawa, Y.; Hoffmann, G.; Blügel, S.; Wiesendanger, R. Spin- and Energy-Dependent Tunneling through a Single Molecule with Intramolecular Spatial Resolution. *Phys. Rev. Lett.* **2010**, *105* (4), 047204. https://doi.org/10.1103/PhysRevLett.105.047204.

(56) Atodiresei, N.; Caciuc, V.; Lazić, P.; Blügel, S. Engineering the Magnetic Properties of Hybrid Organic-Ferromagnetic Interfaces by Molecular Chemical Functionalization. *Phys. Rev. B* **2011**, *84* (17), 172402. https://doi.org/10.1103/PhysRevB.84.172402.

(57) Brede, J.; Atodiresei, N.; Kuck, S.; Lazić, P.; Caciuc, V.; Morikawa, Y.; Hoffmann, G.; Blügel, S.; Wiesendanger, R. Spin- and Energy-Dependent Tunneling through a Single Molecule with Intramolecular Spatial Resolution. *Phys. Rev. Lett.* **2010**, *105* (4), 047204. https://doi.org/10.1103/PhysRevLett.105.047204.

(58) Callsen, M.; Caciuc, V.; Kiselev, N.; Atodiresei, N.; Blügel, S. Magnetic Hardening Induced by Nonmagnetic Organic Molecules. *Phys. Rev. Lett.* **2013**, *111* (10), 106805. https://doi.org/10.1103/PhysRevLett.111.106805.

(59) Friedrich, R.; Caciuc, V.; Kiselev, N. S.; Atodiresei, N.; Blügel, S. Chemically Functionalized Magnetic Exchange Interactions of Hybrid Organic-Ferromagnetic Metal Interfaces. *Phys. Rev. B* **2015**, *91* (11), 115432. https://doi.org/10.1103/PhysRevB.91.115432.

(60) Brede, J.; Atodiresei, N.; Caciuc, V.; Bazarnik, M.; Al-Zubi, A.; Blügel, S.; Wiesendanger, R. Long-Range Magnetic Coupling between Nanoscale Organic–Metal Hybrids Mediated by a Nanoskyrmion Lattice. *Nat. Nanotechnol.* **2014**, *9* (12), 1018–1023. https://doi.org/10.1038/nnano.2014.235.

(61) Friedrich, R.; Caciuc, V.; Atodiresei, N.; Blügel, S. Molecular Induced Skyhook Effect for Magnetic Interlayer Softening. *Phys. Rev. B* **2015**, *92* (19), 195407. https://doi.org/10.1103/PhysRevB.92.195407.

(62) Chua, L. O.; Kang, S. M. Memristive Devices and Systems. *Proc. IEEE* **1976**, *64* (2), 209–223. https://doi.org/10.1109/PROC.1976.10092.

(63) Bandyopadhyay, A.; Sahu, S.; Higuchi, M. Tuning of Nonvolatile Bipolar Memristive Switching in Co(III) Polymer with an Extended Azo Aromatic Ligand. *J. Am. Chem. Soc.* **2011**, *133* (5), 1168–1171. https://doi.org/10.1021/ja106945v.

(64) Nakaya, M.; Tsukamoto, S.; Kuwahara, Y.; Aono, M.; Nakayama, T. Molecular Scale Control of Unbound and Bound C60 for Topochemical Ultradense Data Storage in an Ultrathin C60 Film. *Adv. Mater.* **2010**, *22* (14), 1622–1625. https://doi.org/https://doi.org/10.1002/adma.200902960.

(65) Lee, J.; Chang, H.; Kim, S.; Bang, G. S.; Lee, H. Molecular Monolayer Nonvolatile Memory with Tunable Molecules. *Angew. Chemie Int. Ed.* **2009**, *48* (45), 8501–8504. https://doi.org/https://doi.org/10.1002/anie.200902990.

(66) Quek, S. Y.; Kamenetska, M.; Steigerwald, M. L.; Choi, H. J.; Louie, S. G.; Hybertsen, M. S.; Neaton, J. B.; Venkataraman, L. Mechanically Controlled Binary Conductance Switching of a Single-Molecule Junction. *Nat. Nanotechnol.* **2009**, *4* (4), 230–234. https://doi.org/10.1038/nnano.2009.10.